



Expansion of the spectrum of tumors diagnosed as myxopapillary ependymomas

Fuat Kaan Aras¹ · Dennis Friedel^{1,11} · Felix Keller^{1,2} · Ferdinand Zettl^{1,2} · Rouzbeh Banan^{1,2} · Philipp Sievers^{1,2} · Abigail K. Suwala^{1,2} · Felix Hinz^{1,2} · Lukas Friedrich^{1,2} · Ivan Abdulrazak^{1,2} · Mozhgan Esmaeilbenvidi^{1,2} · Nima Etminan³ · Christel Herold-Mende⁴ · Wolfgang Wick^{5,6,7} · Sandro Krieg⁸ · Stefan M. Pfister^{9,10} · Andrey Korshunov^{1,2} · Isabell Bludau^{1,2} · Felix Sahn^{1,2} · David E. Reuss^{1,2} · Gianluca Sigismondo^{1,2} · Andreas von Deimling^{1,2}

Received: 6 August 2025 / Revised: 18 September 2025 / Accepted: 20 September 2025
© The Author(s) 2025

Both spinal ependymomas (SPE) and myxopapillary ependymomas (MPE) exhibit a characteristic methylation profile [6]. However, for a significant portion of SPE, many pathologists have reported conflicting results between morphologic diagnosis and the DNA methylation-based classification [9, 11]. Indeed, a study by the German Glioma Network reported that nearly one-third of the histologically diagnosed spinal ependymomas were assigned by methylation to the MPE class [14]. In the current study, we address this topic and focus on SPE cases exhibiting a methylation profile of MPE.

We performed immunohistochemical, AI-assisted morphological, as well as methylation analyses on a cohort of 100 MPE and SPE. In addition, mass spectrometry-based proteomic analysis was conducted on 54 of these tumors, including 16 MPE, 23 SPE and 15 discrepant cases. A

detailed description of methods is provided in supplementary materials. Data refinement included filtering for precursor peptides and proteins with q-values > 0.01. Next, low-quality samples with less than 5000 identified proteins were excluded. Additionally, proteins with a high incidence of missing values (i.e., more than 50% in both MPE and SPE) were excluded from the analysis. This approach removed 10 tumor samples, with the final cohort constituting 16 MPE, 17 SPE, and 11 discrepant cases. In these samples, we identified by MS/MS an average of 69,658 (\pm 12,648) peptides and 8029 (\pm 758) proteins per sample at a false discovery rate (FDR) lower than 1% at both peptide and protein level.

Pearson correlation matrix showed higher similarity between discrepant cases and MPEs, compared to discrepant cases and SPEs (Fig. 1). In agreement, principal component analysis (PCA) revealed weakly predominant clustering of

✉ Andreas von Deimling
andreas.vondeimling@med.uni-heidelberg.de

¹ Department of Neuropathology, Institute of Pathology, University Hospital Heidelberg, 69120 Heidelberg, Germany

² Clinical Cooperation Unit Neuropathology, German Consortium for Translational Cancer Research (DKTK), German Cancer Research Center (DKFZ), Heidelberg, Germany

³ Department of Neurosurgery, University Hospital Mannheim, University of Heidelberg, Mannheim, Germany

⁴ Division of Experimental Neurosurgery, Department of Neurosurgery, University Hospital Heidelberg, Heidelberg, Germany

⁵ Department of Neurology, Heidelberg University Hospital, Heidelberg, Germany

⁶ a Partnership Between DKFZ and Heidelberg University Hospital, National Center for Tumor Diseases (NCT), NCT Heidelberg, Heidelberg, Germany

⁷ Clinical Cooperation Unit Neurooncology, German Consortium for Translational Cancer Research (DKTK), German Cancer Research Center (DKFZ), Heidelberg, Germany

⁸ Department of Neurosurgery, Heidelberg University Hospital, Heidelberg, Germany

⁹ Hopp Children's Cancer Center Heidelberg (KiTZ), Heidelberg, Germany

¹⁰ Department of Pediatric Oncology, Hematology, Immunology and Pulmonology, University Hospital Heidelberg, Heidelberg, Germany

¹¹ Faculty of Bioscience, Heidelberg University, 69120 Heidelberg, Germany

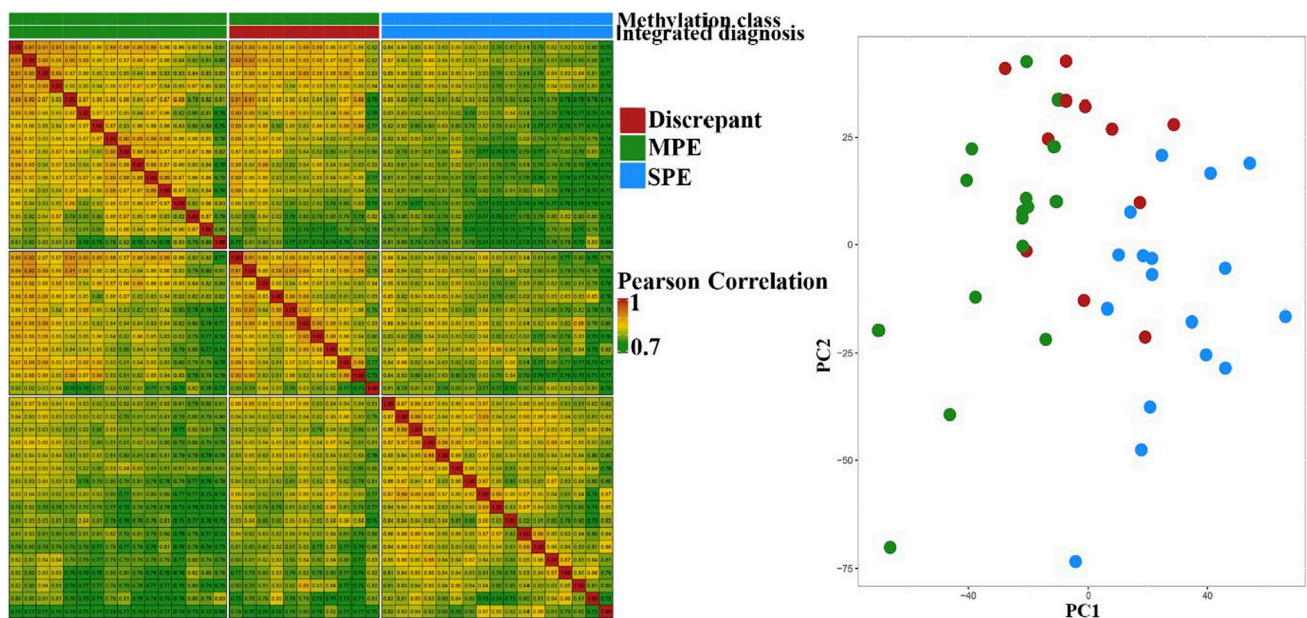


Fig. 1 Pearson correlation matrix (left panel) and principal component analysis (right panel) of proteomes of 44 tumor samples

the discrepant cases with MPEs (Fig. 1). In addition, proteomic analysis identified HOXB13 as the most differentially expressed protein between MPE and SPE. HOXB13 was indeed highly prevalent in all MPEs (16 out of 16 samples) and not identified in any of the SPEs (0 out of 17 samples) (Supplementary Fig. 1). Immunohistochemical staining in a cohort of 100 tumor samples demonstrated 100% sensitivity and 100% specificity (Supplementary Figs. 2 and 3). Differently from previous reports, we did not observe weak or focal staining of HOXB13 in the tumor samples [2, 8, 11, 13]. This can be attributed to the usage of a different antibody compared to previous research (Supplementary Materials). HOXB13 showed strong and diffuse positive staining in all discrepant cases, thus perfectly aligning with proteomic data.

Next, we investigated the morphological features of the cohort. The extracellular proteoglycan versican (VCAN) was overrepresented in the myxoid matrix of MPE (Supplementary Fig. 1). VCAN immunohistochemistry showed excellent alignment with Alcian blue stain; however, VCAN immunohistochemistry demonstrated a more prominent and reliable staining. Employing digital pathology tools and VCAN immunohistochemistry, we demonstrated that discrepant cases frequently contain myxoid *foci* (Supplementary Figs. 4–6 and Supplementary Table 1).

CNV summary plots of MPEs and SPEs were compatible with previous reports [7]. Noteworthy, discrepant cases appeared to exhibit a lower rate of chromosomal aberrations in comparison to MPEs and SPEs. Overall, the summary CNV plot of discrepant cases was more similar to MPE than SPE (Supplementary Fig. 7).

The morphologic and methylation-based classification difference between MPE and SPE has been the subject of several studies [9, 11, 14]. Also, the observation of strong expression of HOXB13 in a fraction of ependymomas with a focus on MPE has been previously reported [2, 3, 5, 8, 11, 13]; thus, our observations corroborate previous reports. As a unique feature, the present study focuses on the conflicting morphological and methylation-based classification of MPE and SPE, while proposing a systematic approach to resolve this discrepancy.

Previous studies observed a differential expression of HOXB13 in morphologically diagnosed MPE [2, 13]. A subsequent study demonstrated strong HOXB13 expression predominantly in MPE, but not in other spinal ependymomas or astrocytomas [8]. After the advent of methylation-based classification, a considerable fraction of morphologically unequivocal SPE produced an mcMPE profile, as reported in several studies [9, 10, 14].

Altogether, the different layers of information demonstrated that discrepant cases show a pattern more similar to MPE than SPE. Our results speak in favor of extending the spectrum of tumors diagnosed as MPE. The diagnosis of an MPE should include the discrepant cases with an SPE-like morphology, but with nuclear expression of HOXB13, and a methylation profile of myxopapillary ependymoma. Adoption of such a pipeline in clinical practice would require modifications of the WHO definition and the essential and desirable diagnostic criteria for these tumors.

It should be noted that cauda equina neuroendocrine tumor, a tumor within the extended differential diagnosis

Essential:
 Glioma with papillary structures and perivascular myxoid change, focal myxoid microcysts or morphological features of spinal ependymoma.
 AND
 Nuclear immunoreactivity for HOXB13
 AND
 Immunoreactivity for GFAP
 AND (for unresolved lesions)
 DNA methylation profile aligned with myxopapillary ependymoma
Desirable:
 Location in the filum terminale or conus medullaris

Fig. 2 Proposal for diagnostic criteria of myxopapillary ependymoma

of MPE and SPE, also exhibits nuclear expression of HOXB13 [1, 4, 12].

We have not observed a classical MPE without strong nuclear HOXB13 expression. We therefore propose classifying tumors that resemble morphologically SPE, but exhibit an mcMPE profile or have nuclear expression of HOXB13 as MPE irrespective of their morphological appearance. This would imply considerable changes to the criteria provided by WHO for the diagnosis of MPE. A suggestion is presented in Fig. 2.

Supplementary Information The online version contains supplementary material available at <https://doi.org/10.1007/s00401-025-02944-w>.

Acknowledgements We acknowledge the support of the university hospital Heidelberg and Mannheim patients and staff in supporting this research. We would like to thank Irina Leis for the immunohistochemical staining of the samples.

Author contributions F.K.A., R.B., D.E.R., G.S., and A.v.D. designed the study. F.K.A., I.A., M.E., and G.S. performed the experiments. F.K.A., D.F., F.K., and F.Z. analyzed the data with contributions from I.B. F.K.A. and D.F. prepared the figures. F.K.A. drafted the article with contributions from all authors. All authors reviewed the manuscript.

Funding Open Access funding enabled and organized by Projekt DEAL. Deutsche Forschungsgemeinschaft, 446166464, 505276113.

Data availability Data are deposited into a public repository for mass spectrometry data (PRIDE, <https://www.ebi.ac.uk/pride/>) and the credentials for access will be shared with the reviewers during revision. Data will be publicly available upon successful acceptance.

Declarations

Conflict of interest The authors declare no competing interests.

Open Access This article is licensed under a Creative Commons Attribution 4.0 International License, which permits use, sharing, adaptation, distribution and reproduction in any medium or format, as long as you give appropriate credit to the original author(s) and the source, provide a link to the Creative Commons licence, and indicate if changes were made. The images or other third party material in this article are

included in the article's Creative Commons licence, unless indicated otherwise in a credit line to the material. If material is not included in the article's Creative Commons licence and your intended use is not permitted by statutory regulation or exceeds the permitted use, you will need to obtain permission directly from the copyright holder. To view a copy of this licence, visit <http://creativecommons.org/licenses/by/4.0/>.

References

1. Asa SL, Mete O, Schüller U et al (2022) Cauda equina neuroendocrine tumors. *Am J Surg Pathol* 47:469–475. <https://doi.org/10.1097/pas.0000000000002009>
2. Barton VN, Danson AM, Kleinschmidt-DeMasters BK et al (2009) Unique molecular characteristics of Pediatric myxopapillary ependymoma. *Brain Pathol* 20:560–570. <https://doi.org/10.1111/j.1750-3639.2009.00333.x>
3. Bockmayr M, Harnisch K, Pohl LC et al (2022) Comprehensive profiling of myxopapillary ependymomas identifies a distinct molecular subtype with relapsing disease. *Neuro-Oncol* 24:1689–1699. <https://doi.org/10.1093/neuonc/noac088>
4. Bockmayr M, Körner M, Schweizer L, Schüller U (2021) Cauda equina paragangliomas express HOXB13. *Neuropathol Appl Neurobiol* 47:889–890. <https://doi.org/10.1111/nan.12713>
5. Bschorer M, Dottermusch M, Matschke J et al (2024) 40-year-old man with two asynchronous spinal cord tumors. *Brain Pathol.* <https://doi.org/10.1111/bpa.13309>
6. Capper D, Jones DTW, Sill M et al (2018) DNA methylation-based classification of central nervous system tumours. *Nature* 555:469–474. <https://doi.org/10.1038/nature26000>
7. Capper D, Stichel D, Sahm F et al (2018) Practical implementation of DNA methylation and copy-number-based CNS tumor diagnostics: the Heidelberg experience. *Acta Neuropathol* 136:181–210. <https://doi.org/10.1007/s00401-018-1879-y>
8. Gu S, Gu W, Shou J et al (2015) The molecular feature of HOX gene family in the intramedullary spinal tumors. *Spine* 42:291–297. <https://doi.org/10.1097/brs.0000000000000889>
9. Kresbach C, Neyazi S, Schüller U (2022) Updates in the classification of ependymal neoplasms: the 2021 WHO classification and beyond. *Brain Pathol.* <https://doi.org/10.1111/bpa.13068>
10. Pajtler KW, Witt H, Sill M et al (2015) Molecular classification of ependymal tumors across all CNS compartments, histopathological grades, and age groups. *Cancer Cell* 27:728–743. <https://doi.org/10.1016/j.ccell.2015.04.002>
11. Purkait S, Praeger S, Felsberg J et al (2025) Strong nuclear expression of HOXB13 is a reliable surrogate marker for DNA methylation profiling to distinguish myxopapillary ependymoma from spinal ependymoma. *Acta Neuropathol.* <https://doi.org/10.1007/s00401-025-02866-7>
12. Soukup J, Manethova M, Stejskal V et al (2023) Immunoreactivity of HOXB13 in neuroendocrine neoplasms is a sensitive and specific marker of rectal well-differentiated neuroendocrine tumors. *Endocr Pathol* 34:333–341. <https://doi.org/10.1007/s12022-023-09779-9>
13. Stephen JH, Sievert AJ, Madsen PJ et al (2012) Spinal cord ependymomas and myxopapillary ependymomas in the first 2 decades of life: a clinicopathological and immunohistochemical characterization of 19 cases. *J Neurosurg Pediatr* 9:646–653. <https://doi.org/10.3171/2012.2.peds11285>
14. Witt H, Gramatzki D, Hentschel B et al (2018) DNA methylation-based classification of ependymomas in adulthood: implications for diagnosis and treatment. *Neuro-Oncol* 20:1616–1624. <https://doi.org/10.1093/neuonc/nyy118>

Publisher's Note Springer Nature remains neutral with regard to jurisdictional claims in published maps and institutional affiliations.